



A Methodology for Supersonic Commercial Market Estimation and Environmental Impact Evaluation (Part II)

Jiajie (Terry) Wen *, Colby J. Weit †, Akshay Anand ‡, Madhukar P. Mayakonda §

Aerospace Systems Design Laboratory at Georgia Tech Lorraine (ASDL@GTL),

International Research Lab Georgia Tech-CNRS, UMI 2958,

Georgia Tech Lorraine, 57070 Metz, France

Turab A. Zaidi ¶

Aerospace Systems Design Laboratory at Georgia Tech Lorraine (ASDL@GTL),

Georgia Tech Lorraine, 57070 Metz, France

and Dimitri N. Mavris ||

Aerospace Systems Design Laboratory (ASDL), School of Aerospace Engineering,

Georgia Institute of Technology, Atlanta, GA, 30332, USA

With the increasing research efforts in civil supersonic transport (SST) during the past decade, companies like Boom and Aerion are making the comeback of civil supersonic flight more promising than ever. Both companies believe that substantial demand exists in civil supersonic aviation, and opportunities are present. However, many regulatory hurdles and operational constraints impose strict limitations on supersonic flight and should not be overlooked. In addition, these aircraft are likely to have higher fuel burn per passenger compared to that for similarly-sized subsonic aircraft, and their effect on fleet-level emissions is unknown. In Part I of this two-part study, the research team successfully demonstrated a methodology that employs a bottom-up approach for estimating the future demand for supersonic commercial operation and its associated fuel burn and CO₂ emission, using only publicly available subsonic baseline-fleet data. This paper seeks to fill the gaps and assumptions identified in the Part I paper by using robust, non-public data, and provides updated results on market estimation and environmental impact (in terms of both CO₂ and NO_x) between 2035 and 2050.

I. Introduction

Even though it has been nearly two decades since the Concorde ceased operations, the desire for civil supersonic flight has never disappeared. The value proposition for these aircraft exists for high-net-worth individuals and business-class travelers who value time savings more than the potential cost associated with supersonic travel. Boom supersonic, a U.S. company developing a Mach 2.2 supersonic airliner, expects a market for up to 2,000 of their 55-seat Overture jets over the decade from the aircraft's anticipated launch in 2023 [1]. Despite the excitement and believed outstanding demand for the revival of supersonic travel, existing constraints and the lack of regulations could impinge the certification of these aircraft and their supersonic flight operations.

These regulatory issues are mainly related to the noise and emissions of civil supersonic aircraft. Aircraft flying supersonically is known to generate an unmistakably loud sonic boom along its flight path, and the sound can be startling and even disturbing for people on the ground. Because of this, the United States [2] (and many other countries) currently has a ban on over-land civil supersonic flights. In addition, the International Civil Aviation Organization (ICAO), the agency responsible for setting standards for global aviation, currently has no provision in its noise certification standard for supersonic aircraft [3].

From a technological standpoint, it is extremely difficult to design a fuel-efficient supersonic airliner. More energy is required to not only accelerate the aircraft to higher speeds, but also to overcome supersonic wave drag and skin

*Researcher, ASDL@GTL and CNRS, UMI 2958, Georgia Tech Lorraine, AIAA Member

†Researcher, ASDL@GTL and CNRS, UMI 2958, Georgia Tech Lorraine, AIAA Member

‡Researcher, ASDL@GTL and CNRS, UMI 2958, Georgia Tech Lorraine, AIAA Member

§Researcher, ASDL@GTL and CNRS, UMI 2958, Georgia Tech Lorraine, AIAA Member

¶Lecturer and Head of ASDL@GTL, Georgia Tech Lorraine, AIAA Member

||S.P. Langley Distinguished Regents Professor and Director, ASDL, School of Aerospace Engineering, Georgia Tech, AIAA Fellow

friction drag during cruise. One study estimated that an SST is likely to burn 5 to 7 times as much fuel per passenger as subsonic aircraft on representative routes [4]. The combustion of jet fuel directly leads to carbon dioxide (CO_2) and nitrogen oxide (NO_x) emissions. The combined effect of commercial supersonic operations with higher fuel burn per passenger on the global scale is unclear. Even though an emission standard for supersonic aircraft currently exists [5], it is outdated and the ICAO Committee on Aviation Environmental Protection (CAEP) Working Group 3 concluded that this standard should not be applied to new engine projects targeting commercial supersonic applications [6].

In Part I of this two-part study [7], the authors noticed that existing studies have investigated SST market and fleet-level environmental impact in isolation, but they have not been coupled together in a traceable, transparent process. To bridge this important gap, the research team first devised a methodology that estimates the global commercial supersonic market by utilizing existing subsonic movement data, then calculates the resulting environmental impact. However, publicly available data is scarce, and a set of enabling assumptions was implemented to generate the market forecast. In Part II of this study, with the help of extensive subsonic movement data acquired from the International Air Transport Association (IATA) [8], some assumptions made in the Part I study are removed. Additionally, a method for estimating full flight NO_x emissions is presented in the environmental impact analysis section.

II. Methodology

A. Challenges Associated with Predicting the Emerging Supersonic Market

A few major challenges were encountered when formulating the methodology that warrants discussion. First, historical data on commercial supersonic operation is sparse. Even though the Concorde was in service for 25 years, it was flown on very limited routes and with low frequency. The Soviet Union's Tu-144 aircraft flew 102 commercial flights, and only 55 of them had passengers aboard [9]. Next, the uncertainty in future policy is high. It is unclear whether the current ban on civil supersonic over-land flight will continue, be lifted completely, or be modified for en-route noise standards. This policy will greatly affect the trajectory of supersonic aircraft and can lower the extent of commercial supersonic service by reducing the number of feasible routes. Lastly, variations in technological advancements and vehicle attributes could also affect commercial supersonic operations and future policy. For example, new aerodynamic design or engine design could allow the aircraft to achieve greater range, enabling the aircraft to operate on more origin-destination (O/D) pairs. The maturity and commercial introduction of low-boom technology [10] can influence the ban on over-land civil supersonic flight.

B. Framework for Market Demand Forecast and Environmental Impact Analysis

After having a basic grasp of the challenges in hand, the next step is to formulate the forecasting methodology that can address those challenges identified. There are two types of commonly used forecasting methods: bottom-up and top-down. The bottom-up approach is typically more granular and rigorous, while the top-down approach offers more flexibility and allows more factors to be considered. For aviation demand forecasting, a bottom-up approach might estimate future traffic demand by analyzing historical data, while a top-down approach is more likely to consider factors such as country GDP, income distribution, and fuel price, etc. To estimate fleet-level emissions, a top-down approach might start the analysis by estimating the number of aircraft in the fleet and their utilization in a given time frame, then calculate the resulting environmental impact. On the other hand, a bottom-up approach might consider the actual routes flown and the frequency of the flights to estimate fleet-level emissions.

Given the scope of the problem at hand, the researchers determined that the bottom-up formulation would be the more appropriate option. Commercial aviation is based on scheduled service with relatively low variability. Traffic movement patterns can be more easily identified for commercial service. Lastly, aircraft utilization (in terms of flight hours per year for example) is usually quite predictable because airlines always try to optimize their schedule and maximize airplane usage. All these factors mean that trends extracted from historical data are more likely to hold in the long term. Once the bottom-up formulation was chosen, the research team then identified three critical elements for quantifying commercial supersonic service demand and its resulting environmental impact:

- Baseline fleet-level data and market forecast
- Development of a supersonic commercial service network
- Fuel burn and environmental impact assessment

Having all three elements in the analysis will ensure a coherent and traceable study. In the following sections, each element will be examined in detail.

III. Subsonic Commercial (Baseline) Fleet-level Data and Market Forecast

A. Global Commercial Aviation Movement Data

As discussed in the Part I paper [7], there are two main reasons for using subsonic movement data as the starting point for estimating supersonic commercial market demand. Historically, supersonic commercial service only provides very limited route choices with low flight frequency, which does not serve as a good reference for future SST operations. Besides, the proposed supersonic commercial aircraft will need to enter the well-established subsonic market and co-exist with the subsonic fleet. Even for O/D pairs with high demand for supersonic service, it is unlikely for SSTs to replace subsonic airliners due to higher predicted ticket costs.

The data used in this Part II study is provided by IATA Market Intelligence Services (MarketIS) [8]. The research team acquired access to data between November 2017 and October 2019. Traffic reports can be generated with different analysis tools provided by the MarketIS infrastructure. For the interests of this study, flight movement data at the origin-destination level from the full year of 2018 is queried for the baseline set of commercial, scheduled operations. Furthermore, the parameters reported for each O/D pair include total passenger count, total revenue, average fare per passenger, total revenue passenger kilometers (RPKs), and yield per passenger kilometer. This data is queried for all global O/Ds in the database and is differentiated by seat class to separate economy and premium class data. The IATA data is built by reported values from a subset of global carriers and scaled to match the estimated global network. The IATA database comprises 7.958 trillion revenue passenger kilometers in 2018 for the global fleet. This number is very close to the Boeing Commercial Market Outlook's estimate of 8.157 trillion RPKs in the same year [11].

Some data pre-processing is required before conducting the analyses. This includes the aforementioned differentiation by seat class and the removal of all O/D pairs that do not report any premium class services. This removal represents an important assumption that no O/Ds without premium class service (business or first class) will have passengers and associated demand willing to pay for a supersonic commercial flight ticket. The resulting set of O/D pairs represents the global aviation network in 2018 that will be used for the forecasting and analysis of future SST network.

B. Forecasting Aviation Growth

Market forecasting is important for stakeholders in the aviation industry to understand future trends of the market. This type of study is typically done annually by aircraft manufacturers such as Airbus [12] and Boeing [11], and the outlook on some of the important indicators such as aircraft delivery, market size, and traffic flow is given in these forecasts. For this study, the traffic volume growth forecast is the most important indicator.

When forecasting growth, region groupings are often introduced to account for the differences in population density, economic development, and other influential factors between any given origin and destination within the global network. For traffic flow forecasting, these region groupings further develop into region pairs. The Boeing Commercial Market Outlook [11] uses 41 distinct region pairs and one to account for the rest of the world, while Airbus Global Market Forecast [12] includes more than 150 total region pairs. Boeing's region pairs and their corresponding growth rates are followed in Part II study because the 42 total region pairs offer a good balance between simplicity and necessary granularity to appropriately differentiate regions. Besides, adhering to Boeing's approach also maintains consistency, since these region pairs and their estimated growth rates were also applied in the Part I study.

IV. Development of Supersonic Commercial Service Network

A. Scenario Generation

Due to the inherent uncertainty when estimating future market growth, this study is conducted with two scenarios in mind, one for high and one for low market demand to capture different possible outcomes of the future supersonic network. As explained in section II.A, one of the major uncertainties that can affect commercial supersonic market demand is the policy on over-land supersonic flight. Most regulations hinge on whether or not SSTs can fly overland supersonically given the sonic boom footprint. However, there is also the potential to consider whether over-land flight is permissible based on underlying population density, such that uninhabited landmasses could be flown over. Non-binary situations are not investigated in the study, because any scenario in-between can be captured by the high and low demand outcomes. As a result, in terms of supersonic flight demand, the binary rule regarding supersonic over-land flight is the major differentiating factor between the two scenarios.

B. Supersonic Flight Routing

For a subsonic aircraft, the ideal flight path typically follows the shortest path on surface between two locations on a sphere, also known as the great circle path. As a result, the flight distance for a subsonic flight is approximately the great circle distance (GCD). For a commercial SST, if supersonic over-land flight is allowed, then the aircraft should also follow the great circle path. However, when over-land flight is impermissible, there are two possibilities: first is to still follow the great circle path, fly faster than Mach 1 only when the aircraft is above water, and decelerate to subsonic speeds before the airplane reaches land; the second approach is to construct a new flight path for each O/D pair based on some criteria to optimize the trajectory. The optimal flight path would depend on the vehicle's performance characteristics and warrant a trade study to be performed. For example, it might be more beneficial in terms of time savings to travel extra distances to extend the duration for supersonic cruise, but this could come at a cost of additional fuel consumption. It is important to achieve a balance between fuel consumption and time savings.

Another consideration for flight path planning is the inclusion of landmass buffer zones to make sure the sonic boom carpet does not reach land areas, even when the aircraft is not flying directly overland. This buffer zone is quite critical, as many cities around the world are located along coastlines. The strength of sonic boom can depend on aircraft design, flight Mach number, aircraft attitude, atmospheric conditions, and many other factors. However, in general sonic boom strength should decrease as the lateral distance from the flight path increases. According to the Concorde flight manual [13], the plane should be flown at least 20 nautical miles (nmi) away from land during level flight, and this distance increases up to 31 nmi when the aircraft is turning at a significant angle.

When the distance between O/D is too far, a re-fuel airport along the way needs to be selected. The proposed SST will have a significantly shorter range than many of the twin-aisle subsonic airliners that it may be competing against for high-paying, long-haul premium class customers. However, an SST could still provide enough time savings even if a re-fuel stop is required. To pick the appropriate re-fueling airport, feasibility in terms of location and infrastructure should both be considered. For example, it would be desirable to limit the great circle distance to a re-fuel airport to be at most a certain percentage less than the range of the vehicle, in case extra distance is required for sonic boom mitigation or diversion due to unexpected events. On the contrary, if the re-fuel stop is too close to the origin or destination airport, it would not make sense from an operational standpoint either. For infrastructure feasibility, the airport needs to satisfy the vehicle's minimum runway length requirement, and it should be able to support civil aviation activities.

Researchers at the Aerospace System Design Laboratory (ASDL) have developed a routing algorithm that can take all the aforementioned considerations into account [14]. It uses a raster-based algorithm called theta-star, derived from the commonly known A-star search algorithm, and modified with Bresenham's Line of Sight algorithm. Two examples of the routes calculated with this algorithm are shown below:

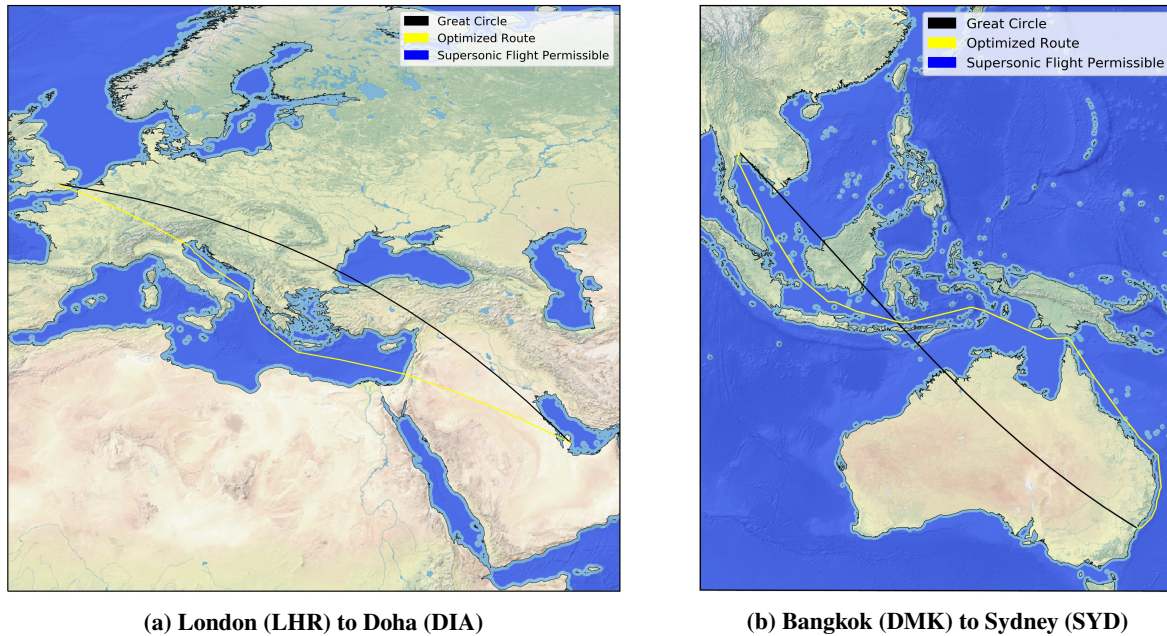


Fig. 1 Great circle and re-routed flight paths generated by the routing algorithm

Since the feasible path from origin to destination is not unique, a cost function needs to be implemented to calculate the "cost" of different routing options. This cost function balances the competing desires of the aircraft to maximize time flying supersonically for time savings but also not diverging too much from an efficient great circle trajectory such that additional fuel penalty is paid. A cost function with higher penalty on fuel consumption might result in a route that has a greater subsonic portion and possibly also fewer accelerations, while a higher time penalty could mean that the aircraft reaches destination faster at the cost of excessive fuel consumption.

$$f(\text{cost}) = \alpha \cdot \text{fuel}_{\text{opt}} + (1 - \alpha) \cdot \text{time}_{\text{opt}} \quad (1)$$

Equation 1 shows the notional version of this cost function. The α parameter creates a scaling between the fuel-optimal and time-optimal solutions to balance these two competing outcomes. The fuel-optimal and time-optimal values are normalized appropriately close to unity in order to enable a meaningful trade between the two trajectory outcomes. More detail on this algorithm and its implementation can be found in a paper by Pfaender et al. that is not yet published (as of the publishing of this paper) [14].

C. Setting the Criteria for Feasibility

Setting the criteria for feasibility and the filtering of feasible routes happens at various stages of data processing. There are three main stages overall: The first stage of filtering is done directly on the subsonic baseline data. Then, more routes are ruled out when they are evaluated with the routing algorithm. Lastly, the list of feasible routes is finalized after a simplified mission analysis. Each of the three stages is discussed in more detail below:

1. Initial Requirements

Starting from the baseline movement data from IATA in 2018, passenger demand data between 2035 and 2050 is forecasted, and preliminary filters are applied to scope down the list of possible origin-destination pairs:

- 1) Great circle distance greater than 1,500 nmi (2,780 km)
- 2) Great circle distance less than 8,100 nmi (15,000 km)
- 3) Enough demand from premium passengers to guarantee four round trips per week

When the GCD is too small, an SST would not be able to bring significant time savings with its additional speed, leading to a non-viable O/D pair. The criterion on maximum distance of the O/D is added because the comprehensive data set from IATA contains O/D pairs with connections that are farther than 8,100 nmi apart. Assuming the SST's range is 4,500 nmi and incorporating a distance buffer to account for the SST needing more than one fuel stop to reach the destination, a route more than 8,100 nmi long is unlikely to be flown. The last filter is related to the demand of premium passengers on current subsonic routes. The authors expect that four round trip flights per week is a reasonable minimum requirement for airlines to consider opening up supersonic service on a new route given the capital intensity of acquiring and operating an SST. However, this requirement of four round trip flights per week for viability can be modified to consider other scenarios. When the aviation industry expands and grows, some routes that don't have adequate demand initially could become viable later down the road, and the forecast of premium class passengers accounts for this reality.

2. Filters Based on Flight Routing Results

The supersonic flight routing algorithm is an essential tool that provides data to help further determine the feasibility of routes. If re-fueling is required, then the selected refuel stop would need to satisfy additional requirements, set for by Pfaender et al. in the routing algorithm capability [14]. The maximum great circle distance from the origin to the re-fuel airport is limited to 4,050 nmi, and the minimum great circle distance from it to the destination is determined to be 1,000 nmi. For infrastructure requirements, the airport should have a minimum runway length of roughly 10,000 ft (9,700 ft was used as a cut-off value to include some airports that are almost 10,000 ft long), assuming that the new SST will be able to land at airports that can accommodate twin-aisle subsonic airliners.

After the required re-fuel stops have been selected, and the optimal path for each O/D pair is determined, the routing algorithm outputs information such as the vehicle speed change as a function of distance and time savings for that route. With these data in hand, the following criteria can then be applied:

- 1) Absolute time savings greater than 1.5 hours
- 2) Relative time savings (time savings relative to overall subsonic trip reference time) greater than 20%
- 3) Total number of subsonic to supersonic accelerations (for each leg of the mission if re-fuel is required) less than 3

The rationales behind the three criteria above have been explained in the Part I paper. Succinctly, the amount of time savings and fuel burn penalties associated with an optimal trajectory must provide enough incentive for passengers to choose that flight over a comparable subsonic flight for the same O/D pair. A re-fuel stop is estimated to take 1.5 hours, and this time penalty is considered when calculating time savings.

3. Feasibility Check Based on Mission Analysis

After the routing algorithm generates the flight path for each O/D pair, a simple mission analysis fuel burn code will check and see whether the aircraft is capable of completing the planned mission. This fuel burn calculation is explained in further detail in section V.

D. Estimating Future Commercial Supersonic Operations

As the previous subsections have described, the original dataset encompassing the global commercial subsonic passenger operations is pared down to a much smaller set of candidate O/D pairs for commercial supersonic operations. The baseline data for 2018 is forecasted to 2050. The most important parameters for demand forecasting are 2018 total estimated passengers at the O/D-level for all fare classes and premium fare classes. The premium fare classes include business and first class, representing the customers most likely to have the willingness to pay for supersonic services and enjoy the benefits of more rapid travel. With the O/D-level passenger data through 2050 for every candidate O/D, the aforementioned criteria are applied to eliminate O/D pairs that do not have appropriate route structure or time savings. Furthermore, this study eliminates O/D pairs without enough passenger demand to support four round trips per week. The remaining O/D pairs are grouped based on the scenario with which they are associated. These groupings are not mutually exclusive, as all of the low-demand scenario O/D pairs are also in the high-demand scenario set.

With the final set of data, the number of SST flights per year in each of the forward forecast years (2025–2050) is computed. 2025 is the estimated year for the new SST's entry to service. The number of flights is directly proportional to the number of premium class passengers expected to demand service within that O/D pair in the forecast year. A switching factor is assumed to estimate what percentage of potential supersonic service customers for that O/D pair will actually fly on an SST instead, i.e., "switching" from subsonic to supersonic. Beyond this, a small increment of induced demand is included to account for passengers that fly supersonic service for novelty or prestige or for frequent fliers who can save enough time to fly more flights than they would have previously. The last element of computing the number of flights is to take the total number of passengers converting to SST services and divide by the number of passengers per flight. The number of passengers per flight is computed by multiplying the number of seats in the potential SST aircraft (assumed to be 55 via the Boom Overture aircraft) by the load factor of an aircraft connecting that region grouping pair (assuming that supersonic load factors are equivalent to the respective subsonic load factor) [15].

Equation 2 represents this computation. The number of SST flights on the O/D pair in year 20XX, #Flights_{20XX}, is equal to the number of estimated premium class passengers in year 20XX, EPP_{20XX}, multiplied by the switching factor, P , divided by the number of passengers per flight, #Seats · LF_{region}. Lastly, this demand is incremented by a small percentage to account for the aforementioned induced demand, ID . The resulting number of SST flights on an O/D pair in year 20XX can be aggregated to calculate the scale of the network as well as to supply inputs for the fuel burn and environmental impact assessment.

$$\#Flights_{20XX} = \frac{EPP_{20XX} \cdot P}{\#Seats \cdot LF_{region}} \cdot (1 + ID) \quad (2)$$

V. Fuel Burn and Environmental Impact Assessment

A. Fuel Burn Analysis

One of the most common methods to calculate mission total fuel burn is to first break down the entire mission into smaller segments, assume the aircraft weight at take-off, and use the Breguet range equation to calculate the fuel required for each segment. They can then be summed to find the fuel burn for a given flight (based on the estimated aircraft weight at take-off). This procedure is then repeated in an iterative process to find the minimum amount of fuel required to complete the mission. The equation below is the Breguet range equation for jet-powered aircraft:

$$R = \frac{V_\infty}{c_f} \frac{L}{D} \ln \left(\frac{W_i}{W_f} \right) \quad (3)$$

In Equation 3, V_∞ is the freestream velocity, and W_i and W_f are the initial and final mass of the aircraft, respectively. To properly estimate mission fuel burn using this equation, lift to drag ratio (L/D) and thrust specific fuel consumption (c_t) of the vehicle at different stages of flight are needed. Since such information on the proposed SST is not available in the public domain, and there is significant uncertainty regarding the performance and efficiency of an aircraft still under development, the research team devised an alternative approach. This simple fuel burn (SFB) method is based on Concorde performance data as well as historic trends, then modified to account for technology improvements. For simplicity, fuel burn during taxiing, transonic deceleration, approach, and landing are neglected, since they typically represent a small portion of the total fuel consumption and will not contribute to substantial differences in this first-order assessment. The fuel burn analysis process has been explained in the Part I paper (Ref. [7]) but elaborated on here to provide extra detail. The same method and vehicle level assumptions are used in this paper as well to ensure consistency. The new SST is estimated to have a maximum take-off weight (MTOW) of 120 tonnes and a maximum fuel weight of 60 tonnes (which includes 6 tonnes of reserve fuel). First, the fuel burn map for the Concorde (processed from the Concorde flight manual) is shown in Table 1 and the fuel burn map for the notional new 55-seat class SST is shown in Table 2.

Table 1 Concorde specific distance maps and acceleration fuel burn

Concorde Subsonic Cruise Climb Specific Distance (nmi/tonne)										
		Normalized Initial Mass								
		55%	60%	65%	70%	75%	80%	85%	90%	95%
Subsonic Cruise Climb Distance (nmi)	500	54.9	51.0	47.5	44.3	41.4	38.8	36.4	34.4	32.7
	1000		53.0	49.4	46.2	43.2	40.5	38.1	36.0	34.1
	1500			51.3	48.1	45.1	42.3	39.8	37.6	35.7
	2000					46.9	44.1	41.6	39.3	37.2
	2500						45.8	43.3	40.9	38.8
	3000							45.0	42.6	40.4
	3500								42.0	

Concorde Supersonic Cruise Climb Specific Distance (nmi/tonne)								
		Normalized Initial Mass						
		55%	60%	65%	70%	75%	80%	85%
Supersonic Cruise Climb Distance (nmi)	500	71.3	65.2	59.9	55.3	51.4	48.2	45.7
	1000		67.4	62.0	57.3	53.2	49.8	47.1
	1500			64.1	59.3	55.1	51.5	48.5
	2000				61.3	57.0	53.3	50.1
	2500				63.3	58.9	55.1	51.8
	3000					60.9	56.9	53.5
	3500							55.3

Concorde Acceleration Fuel Burn (tonne)					
Normalized Initial Mass	59.5%	67.6%	75.7%	83.8%	91.9%
M = 0-0.95	4.0	4.5	5.0	5.5	6.0
M = 0.95-2	11.0	11.8	13.5	14.2	16.0

It should be noted that the values for fuel consumption due to accelerations are much lower for the new SST compared to that for the Concorde. This difference is attributed to the new aircraft being equipped with more fuel-efficient, non-afterburning engines than the Concorde's Olympus 593 engine under high thrust settings. Researchers working on an FAA study at the Georgia Tech Aerospace Systems Design Laboratory have developed a vehicle model for a 55-seat class, Mach 2.2 SST, and the fuel burn results from high-fidelity mission analysis of that vehicle were provided to the research team. These results, coming from a robust vehicle model developed from high-fidelity analysis, are compared to the first-order method results from the fuel burn maps in this study to validate the accuracy of the fuel burn maps. The acceleration fuel burn values are scaled linearly from Concorde's data so that they are similar to the high fidelity method's prediction, otherwise there is no easy way to estimate the fuel burn benefits for a non-afterburning engine design under high thrust settings. The intention here is not to calibrate perfectly this fuel burn method, but rather provide validation for the scaling and assumptions of fuel efficiency improvements made in this study.

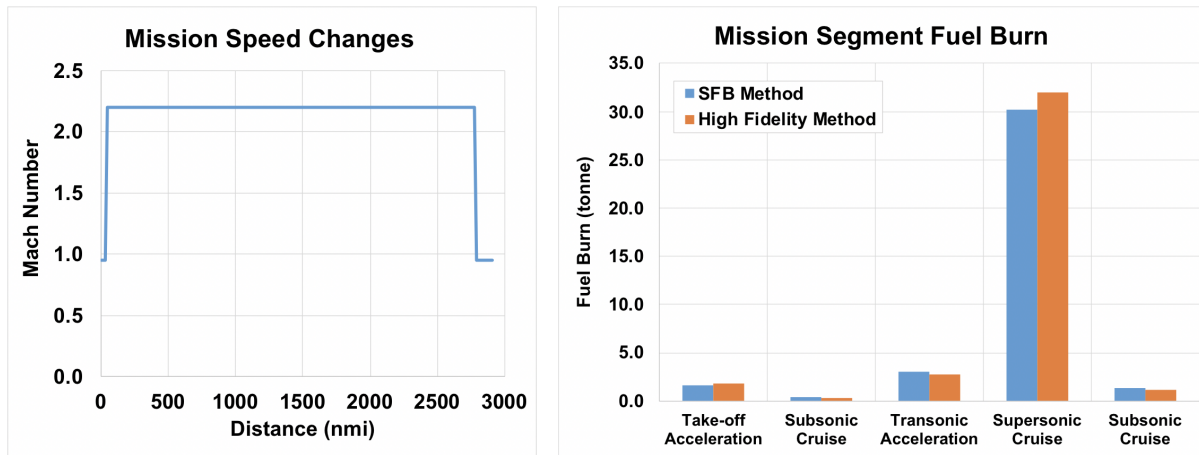
Table 2 New SST specific distance maps and acceleration fuel burn

New SST Subsonic Cruise Climb Specific Distance (nmi/tonne)										
		Normalized Initial Mass								
		55%	60%	65%	70%	75%	80%	85%	90%	95%
Subsonic Cruise Climb Distance (nmi)	500	89.5	85.7	82.1	78.9	76.0	73.4	71.1	69.0	67.3
	1000		87.6	84.1	80.8	77.9	75.2	72.8	70.6	68.7
	1500			86.0	82.7	79.7	76.9	74.5	72.3	70.3
	2000					81.5	78.7	76.2	73.9	71.9
	2500						80.5	77.9	75.6	73.5
	3000							79.6	77.2	75.1
	3500									76.6

New SST Supersonic Cruise Climb Specific Distance (nmi/tonne)								
		Normalized Initial Mass						
		55%	60%	65%	70%	75%	80%	85%
Supersonic Cruise Climb Distance (nmi)	500	104.8	99.3	94.4	90.1	86.4	83.4	81.0
	1000		101.5	96.5	92.1	88.3	85.0	82.4
	1500			98.6	94.1	90.2	86.8	83.9
	2000			100.7	96.2	92.1	88.6	85.6
	2500				98.2	94.1	90.4	87.3
	3000					92.3	89.1	
	3500						90.8	

New SST Acceleration Fuel Burn (tonne)									
Normalized Initial Mass	55%	60%	65%	70%	75%	80%	85%	90%	
M = 0-0.95	1.1	1.2	1.3	1.4	1.5	1.5	1.6	1.7	
M = 0.95-2.2	2.1	2.2	2.4	2.6	2.7	2.9	3.1	3.2	

For the high demand scenario where supersonic over-land flight is permitted, the idealized flight profile is simple and only contains one uninterrupted supersonic cruise segment for one-leg journeys and two for two-leg journeys that require fuel-stops. However, if the over-land flight ban remains effective, then the mission profile would need to be determined by the routing algorithm. Figures 2, 3, and 4 show three example routes for the low demand scenario. The SIN-NRT route in Figure 2 is mainly over water, and the SIN-PER flight path in Figure 3 crosses land once and thus the airplane has to decelerate to subsonic speed and accelerate back to supersonic speed afterward. For the LAX-MIA route in Figure 4, the aircraft takes-off and remains subsonic for more than half of the distance, and accelerates to supersonic speed only after it reaches the Gulf of Mexico.

**Fig. 2** Speed changes and segment fuel burn for Singapore (SIN) to Narita (NRT)

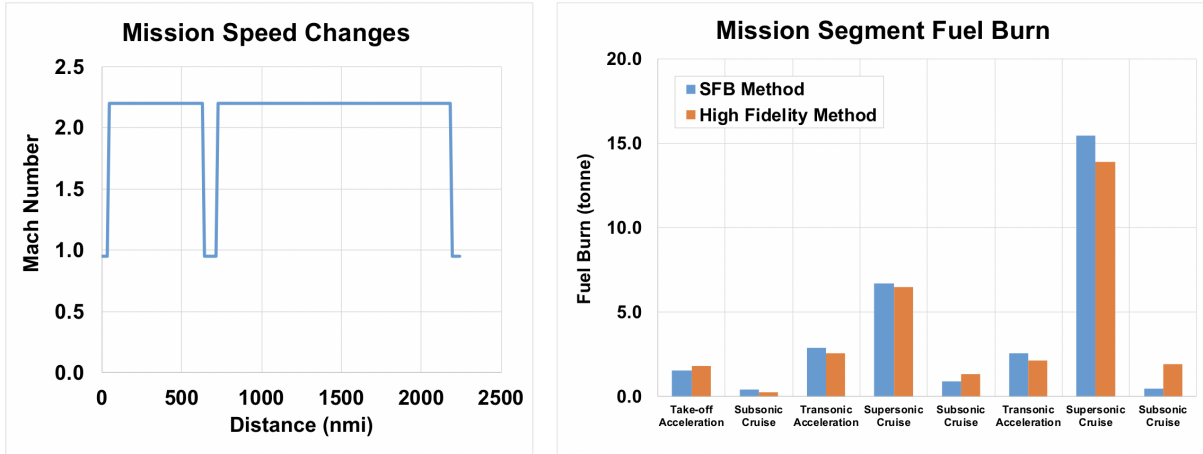


Fig. 3 Speed changes and segment fuel burn for Singapore (SIN) to Perth (PER)

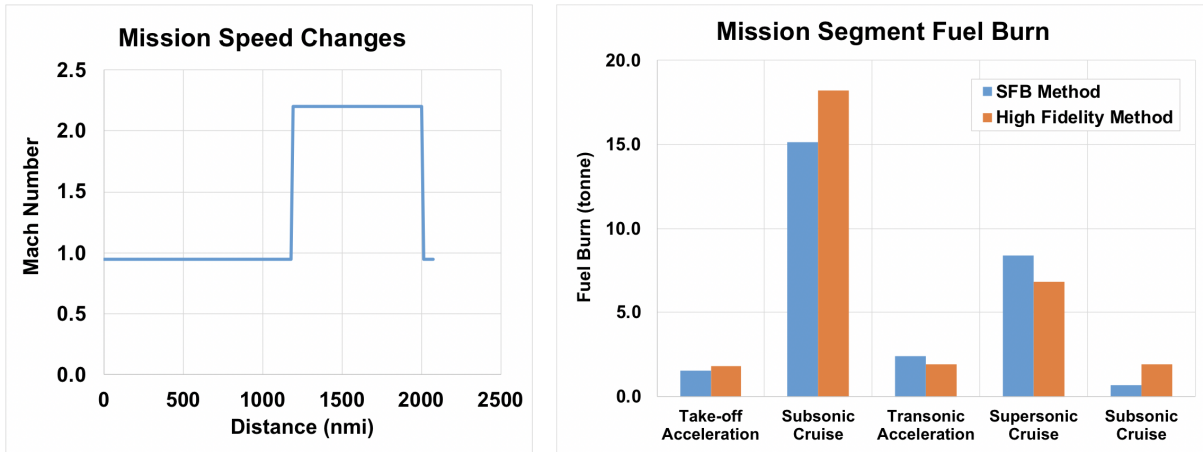


Fig. 4 Speed changes and segment fuel burn for Los Angeles (LAX) to Miami (MIA)

Some observations can be made regarding the differences in fuel burn predictions between the two methods. For example, there is no clear bias for subsonic cruise segments, but the SFB method is likely to yield higher supersonic cruise fuel burn. In addition, fuel burn during transonic acceleration is slightly over-predicted. The mission-level fuel burn provides evidence that the differences are acceptable for a first-order method that does not require non-trivial run-time nor any high fidelity vehicle modeling. With the SFB method, fuel burn is estimated on a large number of routes with minimal computational effort. Table 3 summarizes the results and comparison for the selected routes.

Table 3 Comparison between SFB method and high fidelity method results for mission fuel burn

Flight	SIN-NRT	SIN-PER	LAX-MIA
SFB Method (tonnes)	36.6	31.0	28.2
High Fidelity Method (tonnes)	38.0	30.5	30.7
Difference	3.7%	1.9%	8.3%

With the demand for future commercial supersonic flights estimated and mission fuel burn for each O/D pair for the given scenario (restricted vs. unrestricted supersonic over-land flight) calculated, the mission fuel burn is multiplied by the flight frequency in a given year and aggregated. The sum becomes the predicted fuel consumption of the civil supersonic commercial network for that given year.

B. Carbon Dioxide Emissions

With fuel burn calculated, naturally the next step is to estimate the associated emissions. Carbon dioxide (CO_2) is a byproduct produced during the combustion of hydrocarbon fuel. CO_2 is a common greenhouse gas contributing to climate change, so it is important to estimate the amount of CO_2 produced by supersonic flights on a global scale. For conventional jet fuel, the commonly accepted value for carbon dioxide generated by the aircraft is 3.15 kilograms of CO_2 per kilogram of jet fuel burnt [16, 17]. CO_2 generated by the aircraft engine is typically known as the pump-to-wake CO_2 , or the mobile combustion CO_2 emission factor for jet fuel. This value is only part of the life cycle emission, and the well-to-pump CO_2 emission related to the production of jet fuel is not considered.

C. Nitrogen Oxide Emissions

Carbon dioxide emission is relatively easy to estimate because a majority of the carbon atoms in aircraft CO_2 emissions come from hydrocarbon fuel. However, the nitrogen atoms in NO_x emitted by the aircraft come from N_2 gas in the air. The mass flow rate of air entering the engine varies greatly depending on the operating condition. The commonly accepted approach for estimating N_2 emissions would be to perform engine cycle analysis using a computational program. For example, the Numerical Propulsion System Simulation (NPSS) collaboratively developed by NASA, other government agencies, industry, and universities is capable of this type of task [18]. Since engine cycle modeling is outside of the scope of this study, and uncertainty exists for supersonic engines that are still under development, a simplified approach is needed. The OASyS team decided to estimate the NO_x emission indices (EIs) at the following conditions:

- Landing and Take-off (LTO) Cycle
- Transonic Acceleration
- Supersonic Cruise
- Subsonic Cruise

Continuing the theme of scenario generation, different NO_x emission indices will be used for high and low demand scenarios. One is for the ideal case (lower emissions) and the other is for the realistic case (higher emissions). If demand for SST is high, emission standards are more likely to be more stringent, and manufacturers would need to improve technologies further to lower emissions. Additionally, the emission indices for transonic acceleration and subsonic cruise become especially important for the low-demand scenario, as the vehicle might need to cruise subsonically over-land and perform additional transonic accelerations. The following sections will explain how the NO_x emission indices are estimated for each operating condition.

1. Nitrogen Oxides Emission during Landing and Take-off (LTO) Cycle

Existing regulations can usually provide upper-bound estimates for emissions since newly developed aircraft engines need to comply with more stringent emission standards as technology progresses. Currently, standards on NO_x emissions are only imposed on LTO cycles. Some assumptions need to be made to implement this approach.

LTO cycle emission limits for subsonic aircraft are updated regularly during CAEP meetings, but requirements for supersonic civil aircraft were established in the 1970s and 1980s, and they are now outdated [6]. Using reasonable subsonic LTO cycle NO_x emission limits as a reference is a good starting point. A recent study published by NASA showed that it is technically feasible to design a CFM56-derived supersonic engine and meet CAEP/4 regulation for LTO cycle NO_x emissions [19]. This limit is met by all subsonic turbofan engines produced since 2004. For the ideal scenario, it is assumed that the CAEP/8 limit will be met, representing the current limit for subsonic engines. A 10% margin will be applied during the calculations to make sure the engine emission level stays below the regulatory levels.

In general, these CAEP limits are given in terms of D_p/F_{oo} , which is the mass, in grams (D_p), of the pollutant emitted during a standardized LTO cycle, divided by the rated output (F_{oo}) of the engine. This parameter can be a function of both F_{oo} and π_{oo} , which is the engine's pressure ratio in ISA sea level static conditions [20]. A new 55-seat class commercial SST is expected to have engines with thrust level between 15,000 - 20,000 lbf (67 - 89 kN) [21]. Due to limited amount of publicly available data, F_{oo} of 80kN with a π_{oo} of 15 are assumed for NO_x EI calculations. To get aircraft NO_x emissions per LTO cycle, the value obtained from the ICAO engine emission limit is multiplied by the number of engines on the aircraft, which is assumed to be 3 for this study.

2. Nitrogen Oxide Emissions during Supersonic Cruise

Unfortunately, the same approach cannot be implemented for other flight segments. There are currently no standards in place for subsonic aircraft NO_x emissions during cruise because of the various difficulties associated with measuring emissions in-flight. Additionally, there are no standards on supersonic cruise emissions.

The authors first attempted to implement the Boeing Fuel Flow Method 2 (FFM2) for Estimating Aircraft Emissions [22]. It is a relatively simple method designed to use non-proprietary engine data and no engine model. Instead, it uses ICAO emissions data-bank certification data [20] to correlate thrust level and NO_x EI. This method accounts for pressure, temperature, and compressibility effects at different operating conditions. However, for a vehicle operating at Mach 2.2, this method cannot produce accurate estimates for NO_x EI. As a result, the FFM2 method was used to estimate subsonic cruise and transonic acceleration emissions, which will be explained in the following section. For supersonic cruise, the NO_x EI is simply estimated based on literature.

NO_x EI for Concorde at supersonic cruise condition can be found from various sources [23, 24], and it was even measured experimentally in-flight [25]. For the realistic case, it is assumed that the supersonic cruise emission of a future SST will be just slightly lower than that of the Concorde, and 20 gNO_x/kg_{fuel} was chosen as a reasonable estimate. For the ideal scenario, the EI was decided to be 15 gNO_x/kg_{fuel}, which is comparable to the cruise NO_x EI for a typical subsonic airliner in the 1990s.

3. Nitrogen Oxides Emissions during Subsonic Cruise and Transonic Acceleration

As mentioned previously, the NO_x emission indices during subsonic cruise and transonic acceleration are estimated with the Boeing Fuel Flow Method 2 (FFM2). This method is used because there is no existing NO_x EI data under these conditions, and the lower Mach numbers (or average Mach number for transonic acceleration) allow the FFM2 to produce more accurate estimates.

Based on aircraft engine data compiled by Mattingly [26], the Olympus 593 engine that powered the Concorde has 10,030 lbf of thrust with thrust-specific fuel consumption (TSFC) of 1.190 [(lbm/hr)/lbf] when cruising at Mach 2.0. To estimate the fuel flow rate at subsonic cruise conditions, data provided in Concorde's flight manual [13] is analyzed to gain insight. Figure 5 shows the ratio between fuel flow rate during supersonic cruise at optimal flight level and fuel flow rate during subsonic cruise at various flight levels.

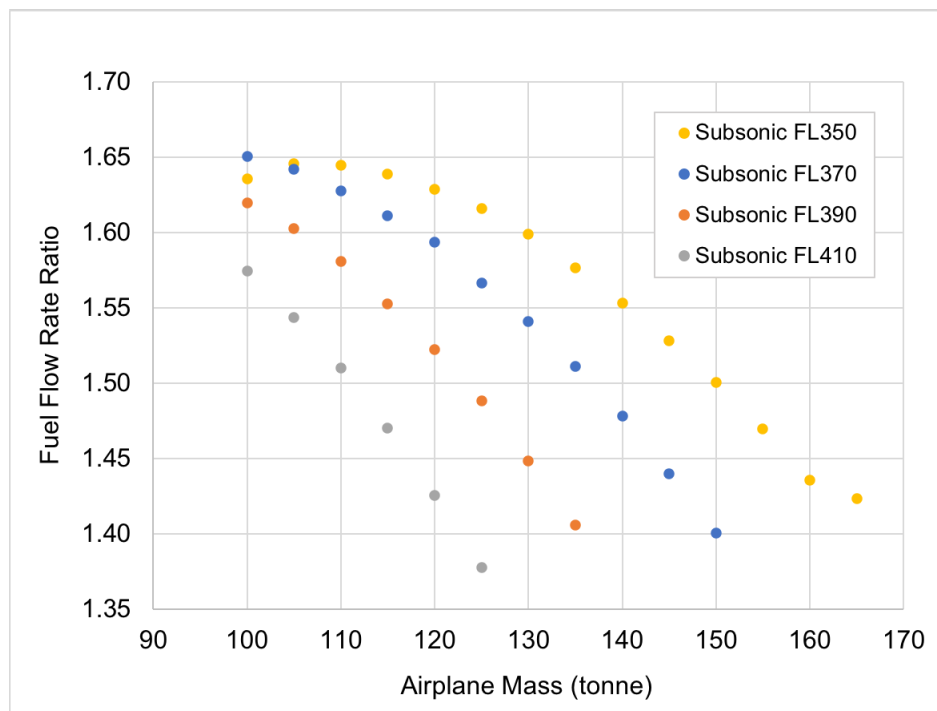


Fig. 5 Fuel flow rate ratio vs. Concorde aircraft mass at various subsonic flight levels

It can be seen that for most cases, the fuel flow rate at subsonic cruise ($M = 0.95$) between flight levels 350 and 410 is between 60%-69% of that for supersonic cruise at the optimal flight level. For this simplified analysis, the fuel flow rate at subsonic cruise is set to 64.5% of that at supersonic cruise, which is 2.14 lbm/s (0.97 kg/s). With the following equation from FFM2, equivalent fuel flow rate at sea level ($W_{f_{SL}}$) can then be estimated with Equation 4.

$$W_{f_{SL}} = W_{f_{Alt}} \frac{\theta_{amb}^{3.8}}{\delta_{amb}} e^{0.2M^2} \quad (4)$$

In Equation 4, θ_{amb} and δ_{amb} are the temperature and pressure ratio at the assumed nominal subsonic cruise altitude of 36,000 ft. Plugging in the appropriate values, $W_{f_{SL}}$ is 1.74 kg/s.

The next step in FFM2 is to correlate this fuel flow rate with NO_x emission indices using data from the ICAO emissions data-bank. To calculate LTO cycle emissions, the engines are tested at four thrust settings corresponding to take-off, climb-out, approach-landing, and taxi/ground idle. Since the Olympus 593 pre-dates ICAO emissions testing, no official data for the Concorde engine is in the data-bank. Additionally, since the Concorde engines used afterburners during take-off and transonic acceleration, the fuel flow rate would be much higher than that for non-afterburning engines. A new commercial SST's engine is most likely to have sea level thrust less than 89kN, but engines in the ICAO data-bank that meet this parameter all have fuel flow rate less than 1.74 kg/s, even at full throttle. Instead of extrapolating values, a non-afterburning, low-bypass turbofan engine with a maximum fuel flow rate greater than 1.74 kg/s at take-off condition is chosen. Engine data from the Kuznetsov NK-86 family meets these criteria and is used. After performing regression at the four certification thrust settings, NO_x emission index for 1.74 kg/s of fuel flow at sea level is 11.7 g NO_x /kg_{fuel}. Finally, ignoring the installation effects and omitting humidity correction, NO_x EI at cruising altitude of 36,000 ft can be estimated using Equation 5. The default value for y is 0.5.

$$EINO_{xAlt} = EINO_{xSL} \left(\frac{\delta_{amb}^{1.02}}{\theta_{amb}^{3.3}} \right)^y \quad (5)$$

Equation 5 gives a final result of 8.7 g NO_x /kg_{fuel}. Comparing to 20 g NO_x /kg_{fuel} for supersonic cruise, this value is slightly higher than expected. However, due to the lack of engine emissions data and engine cycle modeling, this is the best estimate that the research team can provide. According to a NASA contracted study conducted by Boeing in 1989 [27], the NO_x EI for a hypothetical Pratt & Whitney engine powering a Mach 2.4 high-speed civil transport when cruising at Mach 0.9 and 36,000 ft is 7.0 g NO_x /kg_{fuel}.

Lastly, for transonic acceleration, assuming full throttle setting and an average altitude of 45,000 ft, NO_x EI is estimated to be 8.3 g NO_x /kg_{fuel}. Please note that the EI is lower because the effect of lower pressure ratio is greater than the increase in emissions due to a higher thrust setting.

4. Summary of NO_x Emission Indices

Finally, the NO_x emission indices at the four operating conditions are summarized in a tabular format below. Since fuel burn is estimated at various operating conditions for each mission, NO_x emissions can be calculated based on fuel burn for each flight and aggregated on the global level. Subsonic cruise NO_x EI does not need to be considered for the high demand scenario since the aircraft should not cruise subsonically for a significant period of time.

Table 4 Summary of estimated NO_x emission indices for the new Mach 2.2 commercial SST

Operating Condition \ Scenario	Realistic Case - High Emissions (Low Demand Scenario)	Ideal Case - Low Emissions (High Demand Scenario)
LTO Cycle (kg NO_x /LTO)	9.8	7.1
Supersonic Cruise (g NO_x /kg _{fuel})	20	15
Subsonic Cruise (g NO_x /kg _{fuel})	8.7	N/A
Transonic Acceleration (g NO_x /kg _{fuel})	8.3	8.3

VI. Results

In this section, results are reported for both high and low demand scenarios for feasible routes and the number of global, daily supersonic movements between 2035 and 2050. Fleet-level environmental impact for CO₂ and NO_x emissions are also presented. A comparison between the outcomes of Part I of this study, published in Ref. [7], and Part II are provided in the Appendix of this paper.

A. Candidate Routes

After the feasibility criteria explained in section IV.C and region pair growth rates have been applied to the IATA subsonic baseline data, a list of routes feasible for supersonic commercial service can be compiled. Without changing any of the other assumptions, this list can change depending on the forecast year as well as the scenario. Since the number of feasible routes grows with time due to increases in premium passengers, the results shown in this section are for the year 2050. Another important assumption is that having enough premium class passengers to support 4 round-trips per week is the minimum demand requirement for the viability of a route. This assumption is not absolute and can be varied based on the scenario of interest. In 2050 for the high demand scenario, assuming a 100% switching factor, there are a total of 843 feasible routes, and that number drops down to 486 for the low demand scenario. This list of O/D pairs will be referred to as the "candidate routes" or "candidate O/D pairs" in the rest of the paper.

Figure 6 shows the number of candidate routes in 2050 as a function of distance for high and low demand scenarios. The actual list will have fewer routes due to a lower premium passenger switching factor. It can be observed that 30% of the candidate routes in 2050 are between 1,500-2,500 nautical miles for the high demand scenario. Even on longer routes that require re-fuel stops, the SST is still able to make up the time loss due to refueling (assumed to be 1.5 hours) and provide enough time savings by flying supersonically over land.

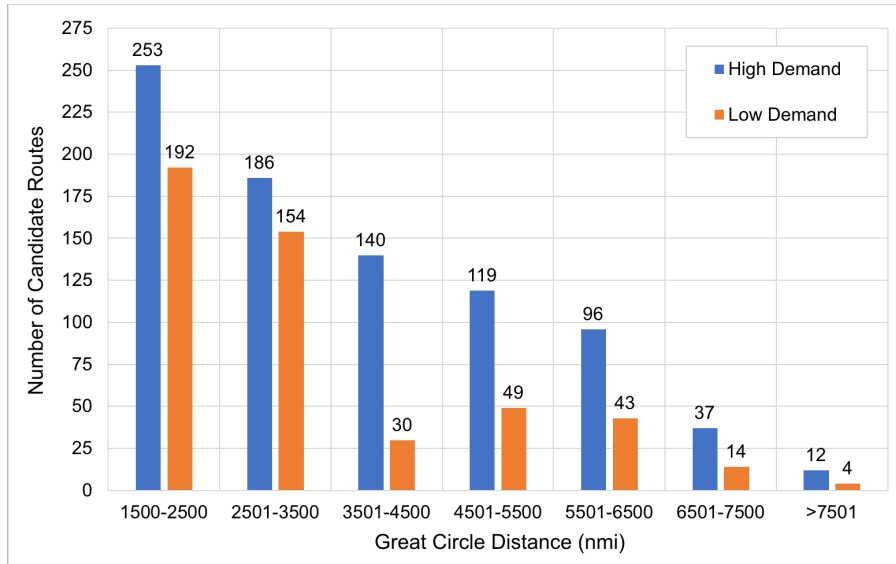


Fig. 6 Number of candidate routes in 2050 as a function of distance for high and low demand scenarios

When supersonic overland flight is not permitted in the low demand scenario, there is a sharp drop in the number of candidate routes, especially those with a distance between 3,500 and 4,500 nautical miles, for two reasons. First, the speed restriction when flying over-land has a noticeable impact on average cruise speed and reduces the speed advantage of the aircraft. Additionally, the re-routed optimal flight path will be longer than the great circle distance, increasing fuel consumption. For some routes this could mean that the SST will no longer be able to complete the flight non-stop. If a fuel stop is added, the time savings could drop below 1.5 hours. For some extreme cases, it would actually be faster to take a subsonic airliner instead. When the origin and destination are really far apart (greater than 7,500 nmi for example), even with a fuel-stop added, the increase in flight distance or number of transonic accelerations due to re-routing could exceed the SST's range capability.

All the candidate routes in 2050 categorized by region groupings are also presented in figure 9 in the Appendix, with the intra-region routes listed before the inter-region routes. Here, flights from A to B and from B to A are grouped

into the same region pair. In this figure, there are not a lot of intra-region routes. This is either because those flights are mostly over-land, or the region simply is not big enough to have many flights above the minimum great circle distance of 1,500 nmi required and provide enough time savings. China has the most intra-region routes for high demand scenario (25 of them), but this number drops down to only 2 if supersonic overland flight is banned. For regions with more ocean coverage such as Oceania and Southeast Asia, the flights are not impacted by this restriction.

Looking at the inter-region routes, there are significantly more candidate routes between Northeast Asia and Southeast Asia than any other region pairs. Due to the geographical advantage in terms of having high ocean coverage in between, supersonic flight restrictions do not render any of those routes infeasible. Europe and the Middle East region pair has the second-highest number of candidate routes, and those flights are not significantly impacted by over-land restriction because they can be re-routed over the Mediterranean sea. On the contrary, flights between China and Europe, the Middle East, and North America are all heavily impacted by overland flight restrictions. For flights from China to Europe and the Middle East, all of them became infeasible because there are no practical ways to re-route them due to the land area in between. The flights between China and North America are unexpectedly reduced between high demand and low demand scenarios. Upon further investigation, a noticeable portion of the routes was dropped because the first leg to a re-fuel airport in Russia requires three accelerations, violating a feasibility requirement. However, the distance is not so far such that the flight can still be completed and the time savings criteria can be met.

B. Demand Estimates

Table 5 shows the daily flight outcomes for the Part II study. These flight numbers include a 1% induced demand increment on total SST demand. The upper and lower bounds of the switching factor for premium class passengers transferring to SST operations are 50% and 10% respectively. The outcomes have a range of 8 to 261 daily flights globally in 2035, and 21 to 667 daily flights globally in 2050. The range of outcomes represents a bounded expectation for the actual outcomes, not a deterministic prediction. The data in the table provides evidence that the low demand scenario leads to a 36% reduction in flights per day in 2035 and a 39% reduction in flights per day in 2050. Rutherford et al. [28] used an assumed 5,000 daily flights per day in the unrestricted (high demand) scenario in 2035. The numbers in Table 5 validate the conclusion found in the Part I study that 5,000 flights per day is an order of magnitude more than expected given the assessment provided in the Part II study.

Table 5 Number of daily flights for year 2035 and 2050

	Year	2035	2050
10% Switching Factor	# Flights per Day (High Demand)	8	34
	# Flights per Day (Low Demand)	8	21
50% Switching Factor	# Flights per Day (High Demand)	261	667
	# Flights per Day (Low Demand)	167	408
<i>Induced Demand: 1% of Total SST Demand</i>			
<i>Round Trips per Week Requirement: 4</i>			

C. Environmental Impact Evaluation

After the flights per year at the O/D-level are forecasted and the fuel burn assessment is completed, the environmental impacts are aggregated from that data. Naturally, fuel consumption is the immediate outcome of the flight movements. Figures 7a and 7b show the consequence of over-land flight restriction on fuel consumption. The additional fuel burn for low demand scenario compared to the high demand scenario is the extra fuel burn for the given route. The data in these figures are collected from the full set of candidates routes for the low demand scenario in 2050. The actual network will be a subset of these routes once all of the demand criteria are applied. This full set of candidate routes is used to illustrate the trends in the low demand scenario data.

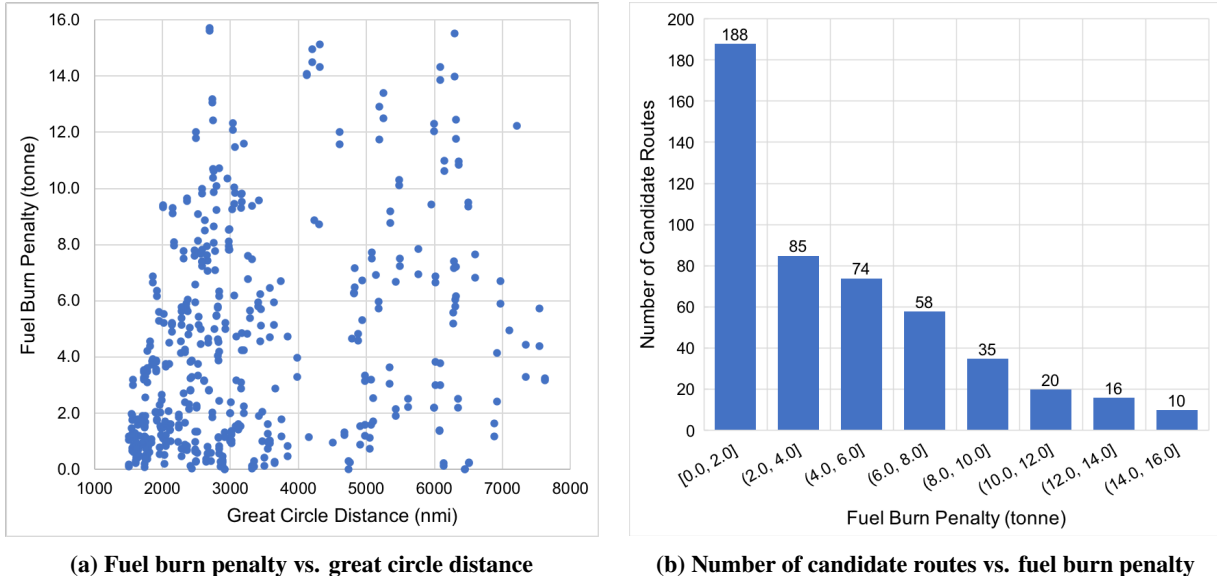


Fig. 7 Fuel burn penalty due to supersonic overland flight restriction for the candidate O/D pairs in 2050

Figure 7a shows that the fuel burn penalty does not necessarily increase with distance between the origin and destination. In fact, there are no clear trends except that data points representing low demand candidate routes are denser when GCD is below 4,000 nmi, and the fuel burn penalties are more skewed toward lower values than routes above 4,000 nmi. Figure 7a confirms that the fuel burn penalty needs to be evaluated on a case-by-case basis, and it is highly dependent on the actual geographical location of the O/D pair. Figure 7b shows the distribution of fuel burn penalty, highlighting that many of the routes that are feasible in the low demand scenario pay a small to moderate penalty to satisfy the over-land restriction requirement.

Figure 8 shows the relationship between fuel burn penalty and time penalty for the low demand scenario candidate O/D pairs, relative to the high demand, unrestricted case. Routes that are mostly over water tend to have low fuel burn penalties and time penalties, which is what one would expect. This scatter plot shows how heavily the routes are affected by the overland supersonic flight restriction. For airlines, operating commercial SSTs on routes represented by data points closer to the origin in this plot might make a more compelling business case.

Fig. 8 Fuel burn penalty vs. time penalty due to supersonic overland flight restriction for the candidate O/D pairs in 2050

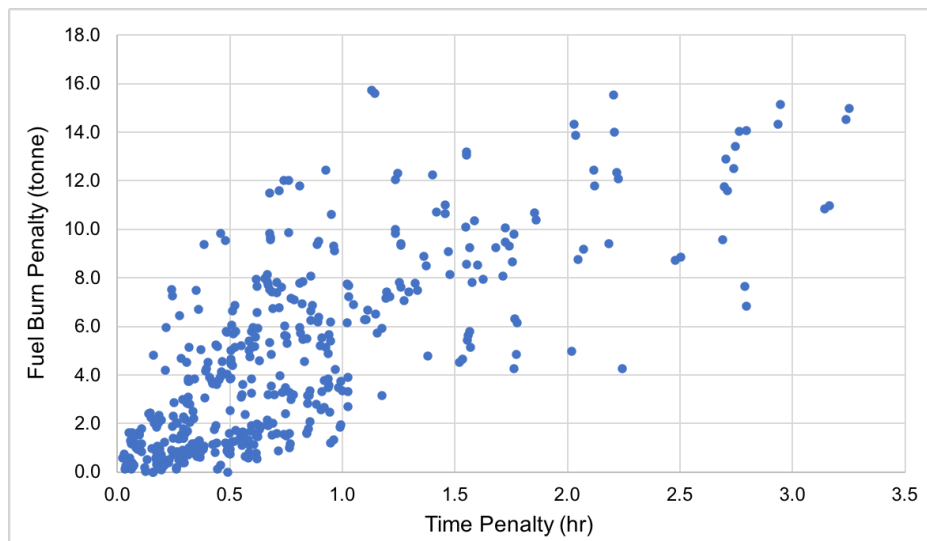


Table 6 shows the CO₂ emissions associated with the expected global daily flights for the different scenarios, switching factor bounds, and forecast years. The values for the 10% switching factor case shown to be a very minimal addition to the existing global aviation CO₂ emissions, adding barely two-tenths of a percent in the highest emission case. For the upper bound 50% switching factor, the CO₂ emissions are significantly higher, with a maximum outcome of 3.63% of 2018 levels in 2050. While the overall magnitudes are quite large in the megatonne range, the addition that SST operations provide to the overall aviation environmental footprint is limited, but not negligible.

Table 6 Global CO₂ emissions and relative CO₂ emissions compared to a 2018 baseline

	Year	2035	2050	Year	2035	2050
10% Switching Factor	CO ₂ Emissions (Megatonne) (High Demand)	0.38	1.66	% Relative CO ₂ Emissions (High Demand)	0.04%	0.18%
	CO ₂ Emissions (Megatonne) (Low Demand)	0.25	0.76	% Relative CO ₂ Emissions (Low Demand)	0.03%	0.08%
50% Switching Factor	CO ₂ Emissions (Megatonne) (High Demand)	13.03	33.29	% Relative CO ₂ Emissions (High Demand)	1.42%	3.63%
	CO ₂ Emissions (Megatonne) (Low Demand)	7.40	18.93	% Relative CO ₂ Emissions (Low Demand)	0.81%	2.06%
<i>Induced Demand Increment: 1% of Total SST Demand</i>						
<i>Round Trip Flights per Week Requirement: 4</i>						
<i>2018 Subsonic Fleet-Level CO₂ Emissions Reference Value: 918 Megatonne</i>						

In addition to the CO₂ outcomes, the full flight fleet-level NO_x emissions is also a meaningful consideration. Table 7 shows the full flight NO_x contributions from the SST network in 2035 and 2050 for both scenarios and the bounds of switching factor outcomes.

Table 7 Global full flight NO_x emissions

	Year	2035	2050
10% Switching Factor	NO _x Emissions (kilotonne) (High Demand)	1.67	7.35
	NO _x Emissions (kilotonne) (Low Demand)	1.33	3.90
50% Switching Factor	NO _x Emissions (kilotonne) (High Demand)	57.47	146.94
	NO _x Emissions (kilotonne) (Low Demand)	38.71	98.76
<i>Induced Demand: 1% of Total SST Demand</i>			
<i>Round Trips per Week Requirement: 4</i>			

According to a report published by ICAO, full-flight NO_x emissions from international aviation in the year 2015 were 2.50 megatonnes [29]. Similar to CO₂ emissions, this represents a small percentage relative to global emissions. The worst-case scenario (high demand with 50% switching percentage in 2050) represents 5.8% of NO_x emissions from international flights in 2015. The non-linear increase in emissions as a function of switching percentage can be observed for both CO₂ and NO_x emissions due to increases in the frequency of flights and route feasibility as demand grows.

VII. Conclusion

A. Summary

In this two-part study, a bottom-up approach has been developed to estimate the market demand for commercial supersonic aviation and its resulting environmental impact. The different subsonic baseline data used in Part I and Part II demonstrated the flexibility and modularity of the market estimation methodology. In the Part II study, non-public subsonic baseline data from IATA is used. The comprehensiveness of the IATA data allows a list of feasible routes at the origin-destination level to be generated in the final result, as opposed to Part I, where producing a detailed list of feasible routes is not possible. One other major addition in the Part II study is the simplified approach for estimating NO_x emission indices and the resulting global full flight NO_x emissions.

B. Further Remarks on the Presented Study

Understanding the assumptions made during the development of this study is very important when analyzing the results presented in this paper. In some sense, the assumptions are more important than the results themselves, since a different set of assumptions will yield different results. By varying different assumptions, the sensitivities of various factors can be better understood, which better informs readers and other stakeholders. The outcomes of this study are presented in wide ranges in an attempt to capture the potential outcome of the future market. The numbers should not be interpreted as deterministic predictions but rather bounds within which the expected outcome is likely to fall.

Assumptions associated with the market estimation process include switching percentage in the range of 10% to 50% and induced demand of 1%. The entry to service for SST is estimated to be in 2025. The passenger load factor on the SST is assumed to be consistent with that for current subsonic airliners, and the percentage varies slightly depending on the region pair. One major assumption removed in this Part II study compared to the Part I study is the percentage of premium passengers. Since the IATA baseline data can provide statistics on this value at the O/D-level, the raw data of premium passengers is used, and an assumption is not needed for the percentage of all passengers that are premium passengers.

Vehicle level assumptions significantly influence the feasibility of routes as well. These assumptions have been discussed in detail in the Part I paper, and the same assumptions are here to maintain consistency. Other assumptions that affect route feasibility include the minimum required premium passenger demand in terms of the number of round trips per week, which is set to four in this study. Last but not least, data referring to the list of candidate routes presented in the results section assume a premium passenger switching factor of 100% to capture as many potential routes as possible.

C. Future Work

The methodology developed in this two-part study does not consider the possibility of new routes being introduced in the future. It could be desirable for airlines to introduce new routes that are favorable for the performance and characteristics of supersonic aircraft. For the percentage of passengers switching to supersonic service, in this study it is simply a variable that gets changed to produce upper and lower bounds of potential outcomes. Since this would be a decision made by potential customers, the authors see the potential to implement a decision-making model based on utility theory and the value of travel time savings to better assess the likely deterministic outcome within the bounds set or to at least narrow the bounds that were set for a higher confidence outcome. In addition, this factor could also increase with time as public acceptance for commercial supersonic service increases. Induced demand is accounted for with a simple percentage increment, but it could be modeled in a more sophisticated manner.

During the route-filtering process, one criterion is that routes in the low demand scenario that require three or more transonic accelerations in one leg will not be considered. This requirement might be too stringent in some cases after evaluating the final list of feasible low demand scenario routes. The minimum number of round-trip flights required per week for an SST route to be viable is assumed to be four in this study, but an economic assessment of a more precise number for that requirement could improve the outcome of the study. Lastly, NO_x estimates can be further refined when better data becomes available for the turbojet engines equipped on SSTs. Additionally, emissions during subsonic climb can be included for more refined estimates. However, it will not have a significant impact on full flight NO_x emissions.

Appendix

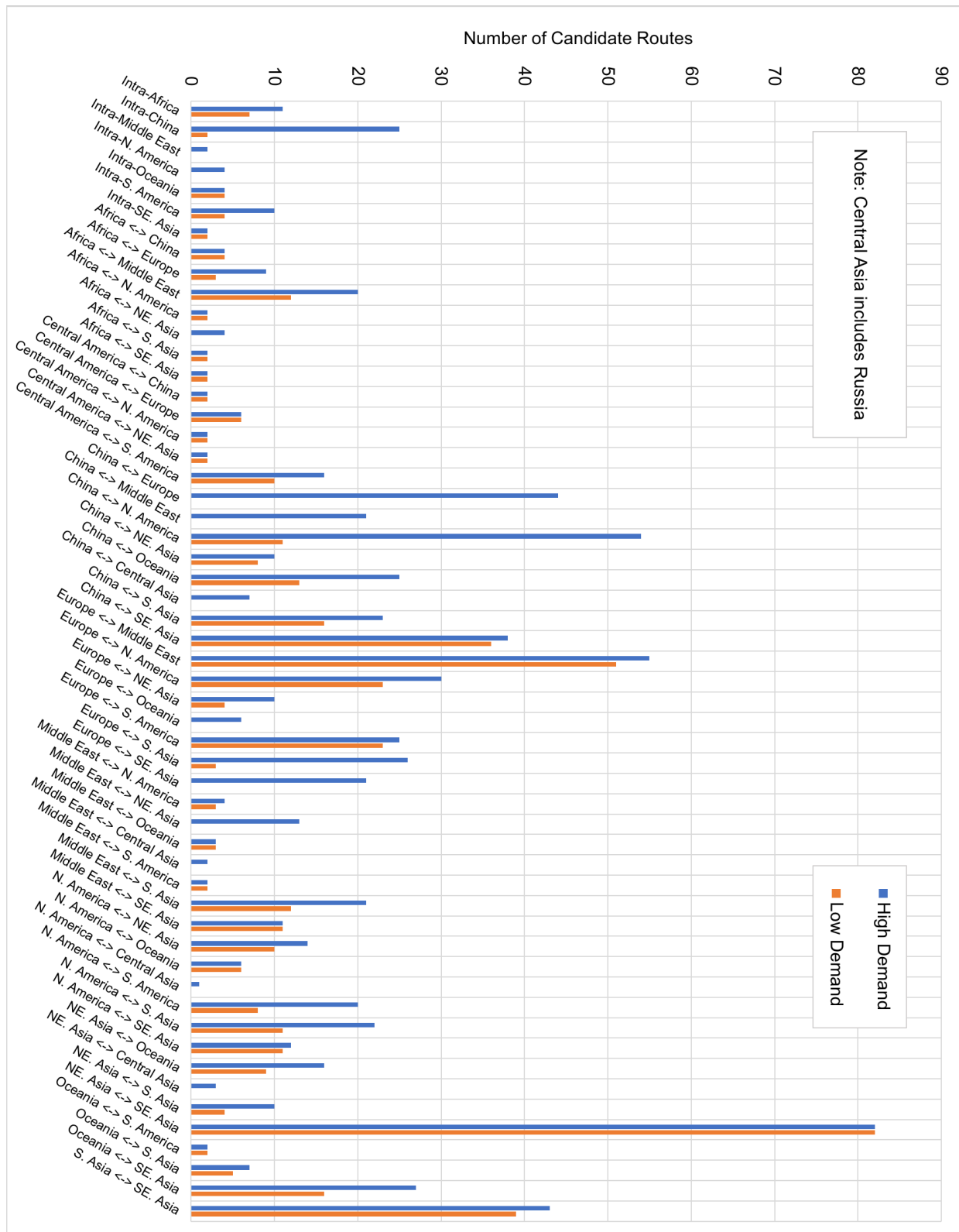


Fig. 9 Number of candidate routes in 2050 for each region pair

Table 8 shows the outcomes of Part I and Part II studies for the number of daily flights in high and low demand scenarios for upper and lower bounds of switching factors. Given that the Part I assessment was revenue passenger kilometer-based rather than origin destination-based, it is not possible to match the assumptions one-for-one to create complete equivalency. The assumptions provided are the best estimate of equivalency, however. The table shows the outcomes similar in order of magnitude but different in absolute numbers. The Part I numbers are all larger than the Part II numbers. Due to the different data sets and assumptions implemented in the same framework of execution, the similarity of the results in order of magnitude is promising. This promise comes from the framework showing its flexibility for the different inputs as well as the results reinforcing each other's limits for upper and lower bound outcomes. It is important not to take these values as a prediction of the specific outcome, but as ranges of potential outcomes. Lastly, this comparison is provided in the Appendix as the outcomes for each study are more important in-and-of themselves than the comparison of those outcomes.

Table 8 Estimated number of daily flights from Part I and Part II studies for 2035 and 2050 forecast years

	Study	Part I		Part II			
		Year	2035	2050	2035	2050	
5% Switching Factor	# Flights per Day (High Demand)	79	118	11	36		
	# Flights per Day (Low Demand)	47	71	7	21		
50% Switching Factor	# Flights per Day (High Demand)	786	1180	520	1134		
	# Flights per Day (Low Demand)	465	711	273	494		
<i>Premium Passenger Percentage</i>		<i>15% (Assumed)</i>		<i>Route-dependent</i>			
<i>Induced Demand Increment (of Total SST Demand)</i>		<i>1%</i>					
<i>Minimum Round Trip Flights per Week Requirement</i>		<i>1</i>					

VIII. Acknowledgments

This project has received funding from the Clean Sky 2 (CS2) Joint Undertaking (JU) under grant agreement No.864521. The JU receives support from the European Union's Horizon 2020 research and innovation programme and the Clean Sky 2 JU members other than the Union. This project was carried out by the Aerospace Systems Design Laboratory at Georgia Tech Lorraine (ASDL@GTL) in Metz, France, under the Georgia Tech – CNRS (Centre National de la Recherche Scientifique) UMI 2958 (Unités Mixtes Internationales) research partnership. The authors dedicate special thanks to Ralf Berghof and Nico Flüthmann of the German Aerospace Center (DLR) for their guidance and support. The authors would also like to express gratitude to members of the OASyS Advisory Board, Dr. Holger Pfaender and Dr. Elena Garcia, for their important contributions. The results and discussion published in this paper are only the views of the authors and do not reflect the views or opinions of DLR nor the CS2JU.



References

- [1] Bogaisky, J., "Boom Raises \$100M To Develop A Supersonic Airliner. It's Going To Need A Whole Lot More." *Forbes Magazine*, 2019.
- [2] "14 CFR §91.817 - Civil Aircraft Sonic Boom." 1989.
- [3] "Annex 16 to the Convention on International Civil Aviation: Volume I, Aircraft Noise," International Civil Aviation Organization, 2008.
- [4] Kharina, A., MacDonald, T., and Rutherford, D., "Environmental Performance of Emerging Supersonic Transport Aircraft," International Council on Clean Transportation, 2018.
- [5] "Annex 16 to the Convention on International Civil Aviation: Volume II, Aircraft Engine Emissions," International Civil Aviation Organization, 2008.
- [6] "Environmental Technical Manual: Volume II Procedures for the Emissions Certification of Aircraft Engines," International Civil Aviation Organization, 2016.
- [7] Weit, C., Wen, J., Anand, A., Mayakonda, M., Zaidi, T., and Mavris, D., "A Methodology for Supersonic Commercial Market Estimation and Environmental Impact Evaluation (Part I)," *SMARTech*, 2020.
- [8] "Market Intelligence Services (MarketIS)," International Air Transport Association, 2020.
- [9] Dowling, S., "The Soviet Union's flawed rival to Concorde," *BBC Future*, 2017.
- [10] Nemec, M., Aftosmis, M., and Spurlock, W., "Minimizing Sonic Boom Through Simulation-Based Design: The X-59 Airplane," National Aeronautics and Space Administration, 2020.
- [11] "Commercial Market Outlook 2019 – 2038," Boeing, 2019.
- [12] "Global Market Forecast, 2019 - 2038," Airbus, 2019.
- [13] "Manuel d'utilisation Concorde, Révision n°.58 du 20 MARS 2003, VOLUME 2," Air France, 2003.
- [14] Pfaender, J. H., "A Modified Path Search Algorithm for Supersonic Flight Mapping (tentative)," *Paper not yet published*, 2020.
- [15] "Healthy Passenger Demand Continues in 2018 with Another Record Load Factor," International Air Transport Association, 2019.
- [16] "IATA Carbon Offset Program - Frequently Asked Questions," International Air Transport Association, 2016.
- [17] "Emission Factors for Greenhouse Gas Inventories," United States Environmental Protection Agency, 2014.
- [18] Lytle, J. K., "The Numerical Propulsion System Simulation: An Overview," National Aeronautics and Space Administration, 2000.
- [19] Berton, J. J., Huff, D. L., Seidel, J. A., and Geiselhart, K. A., "Supersonic Technology Concept Aeroplanes for Environmental Studies," *AIAA SciTech Forum and Exposition*, American Institute of Aeronautics and Astronautics, 2020.
- [20] "ICAO Aircraft Engine Emissions Databank," International Civil Aviation Organization, 2019.
- [21] Trimble, S., "ANALYSIS: JAL invests heavily in supersonic Boom," *FlightGlobal*, 2017.
- [22] DuBois, D., and Paynter, G. C., "Fuel Flow Method2 for Estimating Aircraft Emissions," *Journal of Aerospace*, Vol. 115, 2006, pp. 1–14.
- [23] Rydpal, K., "Aircraft Emissions," *Good Practice Guidance and Uncertainty Management in National Greenhouse Gas Inventories*, International Panel on Climate Change, 2000.
- [24] Houghton, J. T., Meira Filho, L. G., Lim, B., Treanton, K., Mamaty, I., Bonduki, Y., Griggs, D. J., and Callender, B. A., *Revised 1996 IPCC Guidelines for National Greenhouse Gas Inventories: Reference Manual*, Vol. 3, IPCC/OECD/IEA, 1996.
- [25] Fahey, D. W., Keim, E. R., Boering, K. A., Brock, C. A., Wilson, J. C., Jonsson, H. H., Anthony, S., Hanisco, T. F., Wennberg, P. O., Miake-Lye, R. C., J., S. R., Louisnard, N., Woodbridge, E. L., Gao, R. S., Donnelly, S. G., Wamsley, R. C., Del Negro, L. A., Solomon, S., Daube, B. C., Wofsy, S. C., Webster, C. R., May, R. D., Kelly, K. K., Loewenstein, M., Podolske, J. R., and Chan, K. R., "Emission Measurements of the Concorde Supersonic Aircraft in the Lower Stratosphere," *Science, New Series*, Vol. 270, American Association for the Advancement of Science, 1995.

- [26] Mattingly, J. D., and Ohain, H. V., *Elements of Gas Turbine Propulsion*, American Institute of Aeronautics and Astronautics, 2005.
- [27] “NASA Contractor Report 4233: High-Speed Civil Transport Study,” Tech. rep., National Aeronautics and Space Administration, 1989.
- [28] Rutherford, D., Graver, B., and Chen, C., “Noise and Climate Impacts of An Unconstrained Commercial Supersonic Network,” *Working Paper*, 2019.
- [29] Fleming, G. G., and Lépinay, I. d., “Environmental Trends in Aviation to 2050,” Tech. rep., International Civil Aviation Organization, 2019.